The 14th World Conference on Earthquake Engineering
October 12-17, 2008, Beijing, China

FULL DYNAMIC AND PUSHOVER ANALYSES OF OUT-OF-PLANE MASONRY FACADES: APPLICATION AND COMPARISONS BY RBSM

S. Casolo[1] and G. Uva[2]

[1] *Professor, Dept. of Structural Engineering , Politecnico di Milano, Milano, Italy*
[2] *Professor, Dept. ICAR, Politecnico di Bari, Bari, Italy*
Email: siro.casolo@polimi.it,

ABSTRACT :

The paper is focused on the analysis of out–of–plane mechanisms which actually represent the most recurrent collapse mode for the façade of buildings such as churches or basilicas. A full Nonlinear Dynamic (ND) modelling of the seismic response is performed by adopting a specific rigid body and spring model (RBSM), where damage is ascribed to the out-of-plane flexural behaviour. A phenomenological description of the cyclic response of the masonry material is provided in the definition of the constitutive prescriptions, including hysteretic and degrading material behaviour. Then, a comparison is made with a non linear static pushover (NSP) analysis, which is performed by means of the same specific RBSM under quasi-static loading, incrementally applied. The seismic response in terms of generalized force–displacement curve and the ultimate limit displacement capacity are evaluated, comparing them with the seismic displacement demand, expressed in terms of spectral coordinates. The two different approaches are compared by considering as a case study the church of Rosario, in Guastalla, which was damaged by Emilia Romagna Earthquake (1987). A number of analyses have been performed, investigating a variety of different aspects concerning the accelerogram records and their correlation with the damage indicators of the non-linear models.

KEYWORDS: Masonry, out–of–plane behaviour, mechanistic model, dynamics, pushover analysis, Rigid Body and Spring Models

1. INTRODUCTION

Heritage masonry buildings are characterized by a peculiar seismic behaviour very different from that of ordinary masonry constructions, and this requires both the definition of specialized procedures for vulnerability analyses and a careful choice of the significant measures of the seismic action. Accounting for these features is a difficult task, and the urge for effective models suitable for extensive applications can be hardly matched with the unique and unrepeatable character of each single monument.

Actually, typological and semi-empirical techniques that reduce the complex and manifold features of the individual structural response into wide classes do not work so well for monuments as for ordinary buildings [3, 8]. In fact, they are based on the statistical analysis of data obtained from post-earthquake damage surveys, which for monumental buildings are often too scanty. Even when available, the definition of significant vulnerability factors, classes and clear correlation rules is still a controversial matter. Furthermore, the typological features of monuments are extremely variable, and even monuments with similar typological features often show completely different damage patterns.

On the other hand, a mechanistic approach would require an amount of computational resources not commonly available when the investigation of the non-linear response and mechanical degradation of entire masonry buildings is needed. Indeed, in many cases the seismic damage patterns of these structures can be studied by separately considering their different architectural parts. In this sense, a fundamental reference is represented by the works of Giuffrè [7] and Doglioni et al [5], who laid the basis for the study of monumental buildings under horizontal forces by a macro–element approach and the analyses of the most recurrent collapse mechanisms. Thus, it has become a common practice to study the seismic response of limited structural parts and macro–elements instead of modelling the complete building. In any case, for earthquake engineering applications the description of the hysteretic material response and the mechanical degradation under cyclic dynamical loading is paramount. Unfortunately, these models are difficult to handle in a FE context. The mechanistic model adopted in the present paper is based on a specific rigid body and spring approach, which considers only the out-of-plane displacements and assigns hysteretic characteristics to the connection springs in order to approximate the brittle behaviour of masonry material and the degradation due to cyclic loadings [2].

2. THE CASE STUDY

In this paper, attention is focused on churches, which are particularly widespread on the Italian territory, and are the object of a plenty of research studies and applications [5]. For this typology, the experience progressively acquired during post–earthquakes damage surveys reveals that recurrent damage patterns, as well as failure mechanisms, can be identified and classified. This allows to investigate the damage patterns by separately looking to the different parts (nave, aisle, transept, chapel, dome, tower, ...), called macro-elements. The relatively large amount of data collected has been extensively used to establish preliminary relationship between typology and failure mechanism. Unfortunately, such a correspondence is not univocal, and the amount of data is not large enough for a statistical validation of reliable relationships among vulnerability, severity of the ground shaking and level of damage. For all these reasons, it is highly desirable to develop ad hoc mechanical models for the vulnerability assessment of monuments, simple enough to perform a large amount of parametric analyses with a small computational effort, with the aim to predict the most likely failure mechanism that can be activated by an earthquake and the level of ground shaking causing severe structural damage. The damage mechanism that will be here analyzed is the out-of plane collapse of the façade, which is a particularly relevant and recurrent one, and for which a mechanistic model had been specifically formulated [2]. The 17th century church of Rosario at Guastalla (Reggio Emilia, Italy) has been chosen as a significant case study, since is very simple but includes the most important typological features and constructive elements. It has a single nave and a symmetrical façade with a central entrance door and two windows. Façade maximum height is *10.7 m*, width *9.3 m*, lateral wall height *9.0 m*, and the average wall thickness is *0.55 m*. A portion of *7.4 m* of each lateral wall, up to the first lateral chapel, is considered in the numerical model described in the following section..

2.1. The Rigid Body and Spring Model

The proposed mechanistic model [1] assumes that the walls are discretized into plane rigid elements connected to each other in the middle of their adjoining sides by spherical hinges at which all the deformation takes place. In-plane rigidity is assumed, and in general the model is suitable for masonry structures for which shear and membrane effects are negligible compared to flexural, out–of–plane effects, in accord with the hypothesis of Kirchhoff-Love plate. The low strength of the masonry material causes non linearity and damages in the walls remaining in the field of small displacements. The large front wall and lateral walls of a church $\mathcal{B}$ are described in terms of the midsurface $\mathcal{M}$, whose displacements can only be along the out-of plane direction. In the model, the lateral walls, originally perpendicular to the front wall, are rotated so as to be coplanar with it by means of a mapping $\mathcal{M} \to \Omega \subset \mathcal{R}^2$ (fig. 1).

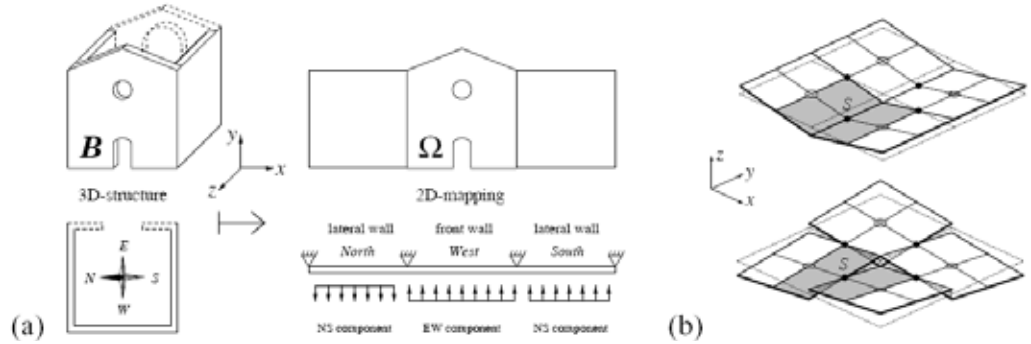

Figure 1 (a) Example of mapping for front wall and lateral walls of a church [4]. (b) Unit cell made by four square elements subjected to pure flexural bending (top), and pure twisting (bottom).

The domain Ω is then partitioned into *m* quadrilateral rigid elements and the joint between a couple of elements, or with a fixed boundary, is modelled as a spherical hinge, placed in the mid-point of the abutting edge, which allows small rotations whose axis is in the plane $z = 0$. Two components of rotation are singled out: one in which the axis is parallel to the edge of the abutting elements (flexural deformation, figure 1–(b), top), and the other whose axis is perpendicular to the edge (twisting deformation, figure 1–(b), bottom). The allowed small displacements *w* of the points on the reference Ω plane are parallel to *z*. The mass of the structure is lumped into the *r* connection nodes. Only two measures of strain are given at each connection joint: the bending curvature χ_f and the twisting curvature χ_t that are assumed as constant in a proper sub-domain associated to each joint. In figure 1–(b), for example, the area relative to the sub-domain associated to

the connection joint S is shaded. The appropriate generalised bending stiffness K_f and twisting stiffness K_t are then assigned to each joint in order to equal the strain energy that corresponds respectively to the deformation fields of bending and twisting of the real structure. The generalised bending and the twisting moment are defined as $b_f = K_f \chi_f$, $b_t = K_t \chi_t$. Such relations can also be extended to the general case irregular quadrilateral elements [1], with an error depending on the geometric distortion. Nevertheless, the approximation is generally good, since the walls of masonry churches can be usually discretized with quite regular elements.

2.2. The Constitutive Model

The elastic-plastic behaviour of the connection joints under cyclic loading is modelled by adopting a phenomenological approach. The most important features of the constitutive relation are shown in figure 2(a).

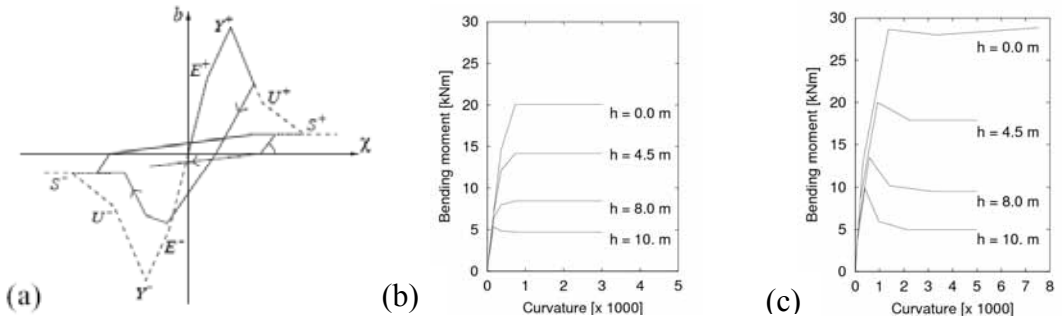

Figure 2 (a) Hysteretic behaviour of the connection joint [2]. (b) First loading skeleton curve for horizontal hinges at different heights. (c) First loading skeleton curve for vertical hinges at different heights.

The points that define the skeleton curve $S^-U^-Y^-E^-OE^+Y^+U^+S^+$ (Fig. 2a) for the flexural behaviour are analytically evaluated using a fiber model at the cross–sectional level of the plate–wall. According with the orthotropy, different values are assigned to the connection joints depending on the orientation of the corresponding edge.

It is assumed that the hysteretic behaviour related to flexural bending is independent of that related to twisting. The following linear formulas for the flexural strength and the twisting strength of a connection joint with the edge inclined at an angle θ (in radians) are assumed: $b_f^{\theta} = 2/\pi\,(b_f^v - b_f^h)\;\theta + b_f^h$; $\quad b_t^{\theta} = 1/2\,(b_f^v - b_f^h)$.

More specifically, with regard to the horizontal hinges, the bending strength is related to the compression due to the vertical gravity load, as shown in figure 2(b), and reflects the circumstance that the horizontal contact surfaces are subjected to combined compressive and bending stress (fig. 3a). Instead, the fiber model of the vertical hinges (fig. 2c) accounts for the interlocking effect occurring within the masonry (fig. 3b), as a function of the frictional contribution under vertical gravity loads, and of a "shape" factor expressing the quality of the masonry texture as a function of the blocks' aspect ratio and their stagger (fig. 3b).

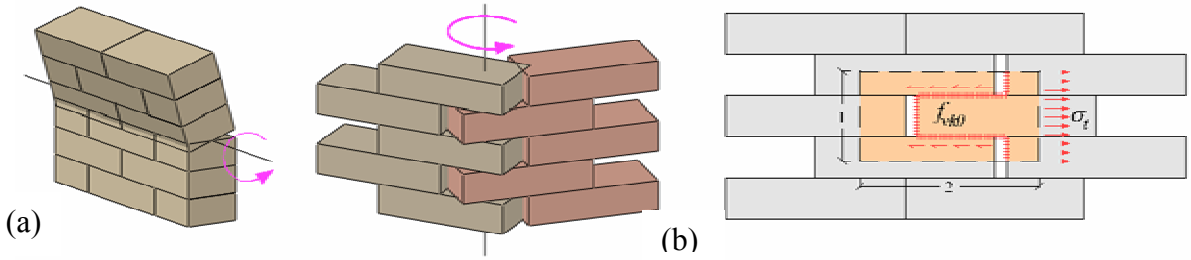

Figure 3 (a), connection joints and points used for the displacement control. (b) Parameters involved in the evaluation of the interlocking effect for the vertical hinges

The basic mechanical parameters assumed as a reference for the analyses are the characteristic initial shear strength of masonry, under zero compressive stress (f_{vko}=*0,05 N/mm*^{2}); the characteristic compressive strength of masonry (f_{ck}=*1,5 N/mm*^{2}) and the characteristic tensile strength of mortar (f_{tk}=*0,005 N/mm*^{2}). The skeleton curve, the stiffness and the strength decay depending on the maximum positive and maximum negative curvatures reached during the loading history (fig. 2a). In order to damp the higher modes, algorithmic damping is introduced by properly choosing the

parameters of implicit integration. The implicit method of Newmark is adopted to integrate the system of equations of the motion, performing full Newton-Raphson iterations until convergence is attained. The mesh of the discrete model, made by *80* rigid elements and with a total number of *78* degrees of freedom is shown in figure 6a.

3. NON LINEAR DYNAMIC VS NONLINEAR STATIC ANALYSIS

Step–by–step nonlinear dynamic analysis is hardly used in the practical application, although it is definitely the most complete and realistic approach for seismic analysis. Indeed, it presents a number of drawbacks, which actually restrict its use to advanced users and very specific case studies: adequate numerical codes – even commercial ones – are not easy available, or introduce too many complications for average end–user; the definition of the model, especially with regard to the constitutive aspects (the post–elastic, hysteretic behaviour of the structure, and the consequent energy dissipation, should be consistently reproduced) is critical; the choice of significant input accelerograms is still a controversial question; the computational cost is very high; the uncertainty about input data strongly influence the reliability of the results. Anyway, in order to predict the nonlinear structural response under strong ground motions, in the last few years simplified procedures have been proposed aimed at performing non linear analysis in a static context (Nonlinear Static Procedures - NSP), where the problem can be more easily managed, and numerical tools with a high circulation are available. These methods, generally known as *pushover* analyses, have recently assumed a large relevance, especially for the assessment of existing buildings [10]. In these procedures, basically, a computational model of the structure is loaded up with a proper distribution of horizontal static loads, which are gradually increased with the aim of "pushing" the structure into the nonlinear field. The basic idea is that the resulting response conveniently represents the envelope of all the possible structural responses, and can so be used to replace a full nonlinear dynamic analysis. When speaking of historical and monumental buildings, the question is even more critical: nearly all the structural analysis methods suffer from a lot of uncertainties and limitations, mainly derived from the incompleteness of the knowledge level, from the presence of widespread inhomogeneities and nonlinearities, and a complex constructive history.

3.1. Nonlinear Dynamic analyses with design–consistent artificial accelerograms

In order to perform the full dynamic analyses, a set of at least 3 accelerograms must be used which should be consistent with the design spectrum. In the case study, a group of 6 artificially generated accelerograms was used, consistent with the design spectra of the zones 1, 2, 3 and 4 in which the Italian territory is classified (an "A"–type soil and a return period of *475* years have been considered). Then, for each isoprobable spectrum, 6 accelerograms were generated according with the procedure and the attenuation law proposed by Sabetta and Pugliese [9].

Table 3.1 Results of the NLD analyses

	ZONE 1		ZONE 2		ZONE 3		ZONE 4	
	d_{max}	$\Delta T\%$	d_{max}	$\Delta T\%$	d_{max}	$\Delta T\%$	d_{max}	$\Delta T\%$
#1	collapse		collapse		0,375	12,41%	0,136	2,53%
#2	collapse		collapse		0,368	12,49%	0,1357	2,48%
#3	collapse		collapse		0,390	13,68%	0,133	2,65%
#4	collapse		collapse		0,330	12,19%	0,1316	2,21%
#5	collapse		collapse		0,388	13,12%	0,1329	2,26%
#6	collapse		collapse		0,403	13,79%	0,1178	1,96%
#7	collapse		collapse		0,386	12,00%	0,1296	2,11%
#8	collapse		0,664	31,68%	0,335	12,47%	0,1283	2,15%
#9	collapse		0,649	29,73%	0,366	13,49%	0,1254	2,36%
#10	collapse		0,574	25,51%	0,384	13,25%	0,1312	2,17%
#11	collapse		0,692	32,77%	0,372	13,87%	0,1187	2,04%
#12	collapse		0,758	31,64%	0,360	14,02%	0,114	1,82%
Mean value	-	-	0,6672	30,27%	0,372	13,07%	0,1279	2,23%
Std deviation	-	-	0,0599	2,573%	0,0208	0,689%	0,0070	0,234%

The global behaviour of the discrete model of the façades and lateral walls is summarized by means of two response

indices that can be related with the structural degradation. The first response index is given by the maximum mean displacement attained during the time history response. The second response index compares the 1^{st} natural period at the end of the time history T^f, evaluated on the basis of the secant stiffness, with the initial period T^i: $\Delta T\% = (T^f - T^i)/T^i$ and represents the average elongation percentage of the 1^{st} natural period. This index is proportional to the global stiffness degradation and, moreover, is also related with the maximum deformation attained during the whole time history.
For each seismic zone, 12 accelerograms have been used to perform the NLD analyses, and the results are summarized in table 3.1. It should be remarked that all the analyses performed with the accelerograms corresponding to the Zone 1 failed, indicating that the collapse of the façade occurs. For Zone 2, only 5 analyses were successful, and the mean values calculated are therefore referred on this limited sample.

3.2. The pushover simulation

The non linear static analysis of the church's façade is now proposed, following the methods included in the european codes [10], which are based on the well–known "N2 method" [4, 6]. The aim is to perform a critical comparison with the full dynamic analysis, appraising the reliability and relevance of the results and assessing the actual advantages that can be obtained.
Analyses were performed by applying two different vertical distributions of the lateral loads: a "uniform" pattern, based on lateral forces that are proportional to mass regardless of elevation (uniform response acceleration); a "modal" pattern, proportional to the 1st modal shape.
The final output of the pushover analysis is represented by a generalized force–displacement relationship: F_b-d_c, where the base reaction is plotted against the displacement of a representative point. The process is carried on until the "ultimate limit condition" of the structure is reached.
The ultimate limit state verification then consists in checking out that the ultimate displacement capacity is larger than the corresponding displacement required by the design seismic action. It is hardly worth observing that in order to perform a nonlinear analysis, even if a static one, a proper numerical code is needed (for instance, a FE code) as well as nonlinear constitutive laws for the materials and the structural elements, able to reproduce the strength and stiffness degradation suffered by the damaged elements. Indeed, the idea of handling a nonlinear static analysis in order to take into account –at least in a simplified way– the inelastic characteristic of the structure was suggested by the availability of codes able to provide these kind of models, whereas the requirements for dynamic analyses are rather oriented to specialist users. It should be anyhow remarked that some operational drawbacks still exist, and even in the most advanced numerical formulations, it is frequent to encounter troubles in the reconstruction of the equilibrium path.
In the case study, the pushover analyses were carried out by using the RSBM described in Par. 2.1. The average value of points A,B,C,D shown in figure 5 a is the characteristic displacement d_c chosen in order to monitor the structure and trace the pushover curve in terms of the equivalent lateral force F_b. Whereas representing the capacity of the structure, it should be compared with the seismic demand provided by the design spectrum.
The methodology includes the following steps: *i)* transformation of the pushover curve into a simplified bilinear force-displacement relationship for an equivalent SDOF system; *ii)* definition of the inelastic seismic demand for such SDOF system in the acceleration–displacement (AD) format; *iii)* transformation of the displacement demand (i.e. the "target" displacement) for the SDOF system into the corresponding maximum displacement of the original structure; *iv)* verification of displacement compatibility (according to the current standards, for masonry structures only the global displacement checking is required, and not a specific assessment of single structural elements).
At the collapse point of each curve, the damage pattern of the façade was drawn, and the damage index $\Delta T\%$ was calculated. This information allowed to perform a critical comparison with the ND analyses.
In figure 5b, the curve expressing the base reactions F_b vs the characteristic displacement d_c of the façade is shown for the two considered loading patterns (mode 1 – horizontal loads proportional to the first modal shape; mode 0 - uniform pattern) together with the force–displacement (F^*–d^*) relationship for the SDOF equivalent system, obtained by applying the modal participation factor Γ:

$$F^* = \frac{F_b}{\Gamma} \qquad d^* = \frac{d_c}{\Gamma} \qquad \Gamma = \frac{\sum m_i \phi_i}{\sum m_i \phi_i^2} = 1.205 \tag{3.1}$$

(Φ is the 1^{st} modal shape of the structure, with $T=0.198\ s$).

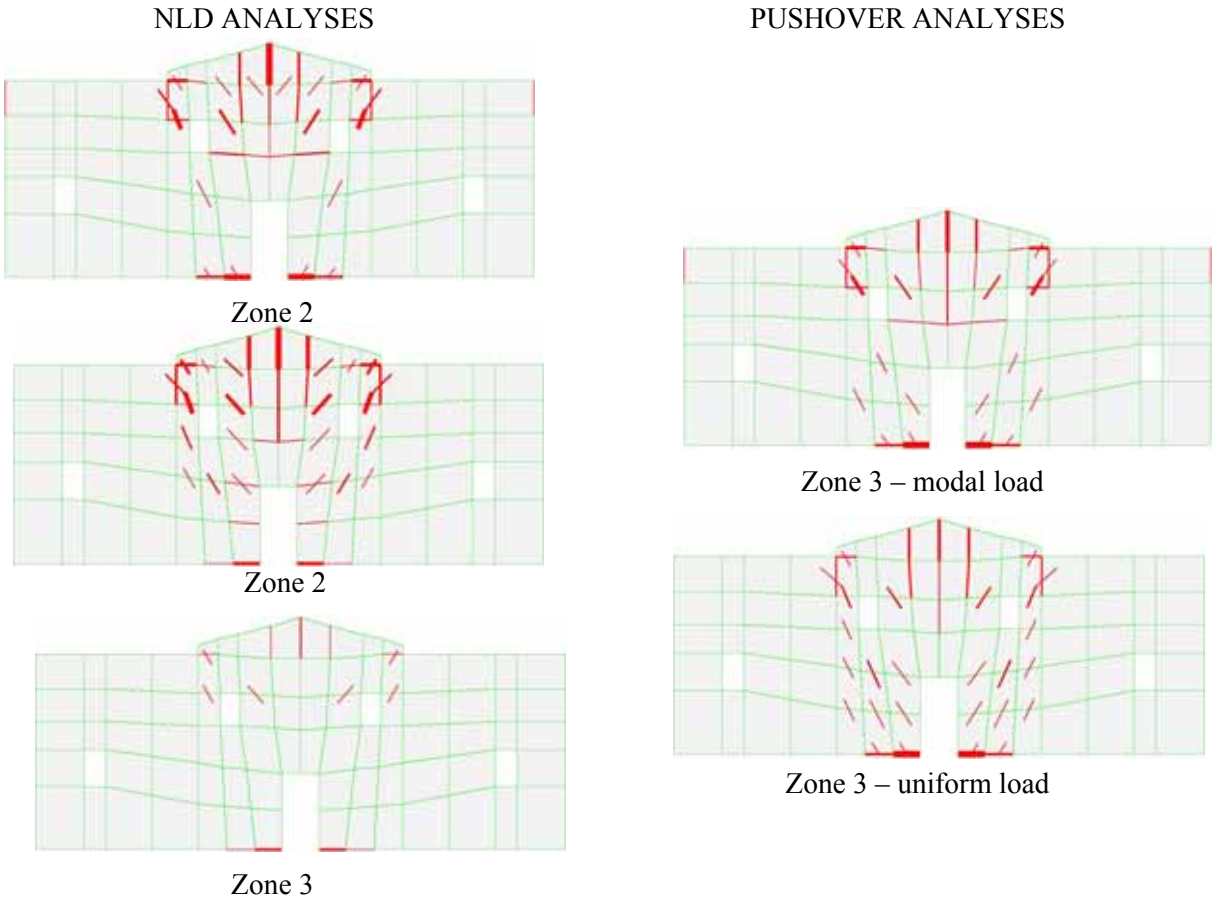

Figure 4 Comparison among the damage patterns for the church's façade: on the left, the ND results; on the right, the "pushover" results. In the center, the color scale for the max curvatures attained at the connection lines.

The characteristic curves F^*–d^* were then transformed into a bilinear simplified relationship also plotted in figure 5b, obtaining the yield forces $F^*_{y1} = 202\ KN$, $F^*_{y0} = 261\ KN$; the ultimate displacements $d^*_{max\ 1}=0.68\ cm$, $d^*_{max\ 1}=0.56\ cm$ and the displacement at yielding $d^*_{y1} = 0.523cm$, $d^*_{y0} = 0.459cm$ (transformation is based on an equal–energy criterion).
At this point, the actual seismic demand for the inelastic system is needed. The procedure can be graphically visualized in AD format, as illustrated in figure 6, where both the demand spectrum and the capacity diagram are plotted together. The elastic design spectrum in AD format is a parametric function of the natural period T^*: ($S_{de}(T^*)$, $S_{ae}(T^*)$). Thence, for the idealized bilinear system ($T^*=0.223\ s$, $m^*=\Sigma m_i \Phi_i$), the acceleration demand (strength) in the case of a perfectly elastic behaviour, and the corresponding elastic displacement demand, can be singled out. The inelastic seismic demand is henceforth defined by accounting for the system ductility, depending on the range of the spectrum in which the system's period falls. The watershed is represented by the characteristic period of the ground motion T_C, defined as the transition period from the constant acceleration branch of the spectrum to the constant velocity one. In this last segment, the equal displacement rule applies: if $T^* \geq T_C$, the inelastic displacement demand $S_d(T^*)$ is assumed to be the same as the elastic system having the same period: $d^*_{max} = d^*_{e\ max} = S_{de}(T^*)$, where $S_{de}(T^*) = S_{ae}(T^*)\ (T^*/2\pi)^2$. If $T^* \leq T_C$, instead, and that's the case, the displacement response of the inelastic system is larger than the equal period elastic one, and can be evaluated by the following expression:

$$d^*_{max} = \frac{d^*_{e\ max}}{q^*}\left(1+(q^*-1)\frac{T^*}{T_C}\right) \geq d^*_{e\ max} \qquad \text{where} \qquad q^* = S_{ae}(T^*)\frac{m^*}{F_y} \tag{3.2}$$

The factor q^* represents the ratio between the force corresponding to a linear elastic response and the yielding force of the equivalent system (it will be always assumed $q^* \geq 1$).

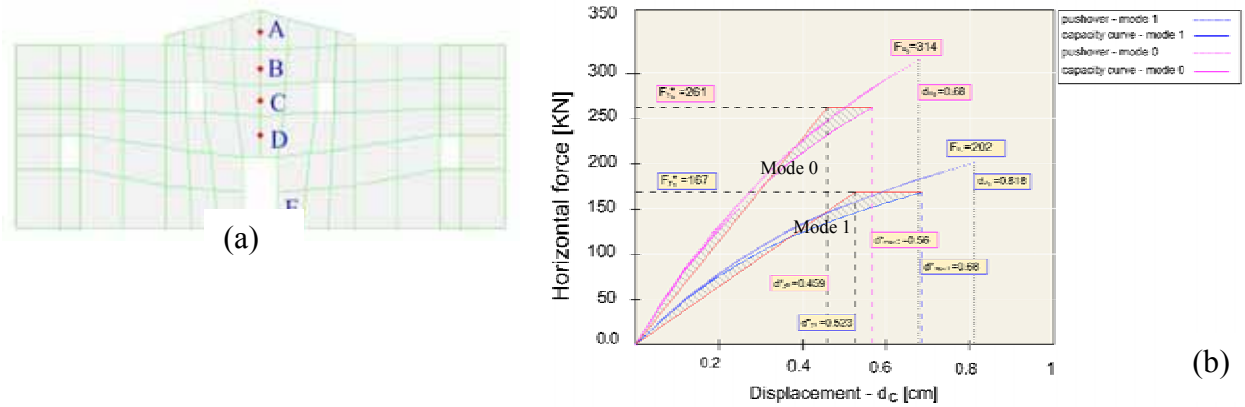

Figure 5 (a) Loading histories for the Pushover simulations; (b) Pushover and capacity curves for the church façade

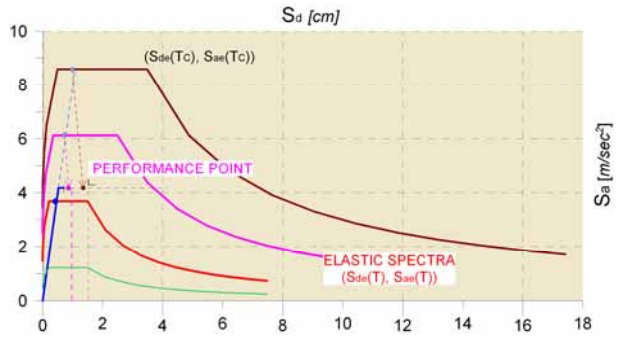

Mode 1					
	Zone 1	*Zone 2*	*Zone 3*	*Zone 4*	unit
$S_{ae}(T^*)$	8.58	6.13	3.68	1.23	*[m/s²]*
q^*	2.06	1.472	1.00	1.00	
$d^*_{e\,max}$	1.080	0.771	0.463	0.154	*[cm]*
d_{max}	1.834	1.167	**0.558**	**0.186**	*[cm]*
$\boldsymbol{d_u}$			**0.818**		*[cm]*
Mode 0					
	Zone 1	*Zone 2*	*Zone 3*	*Zone 4*	unit
$S_{ae}(T^*)$	8.58	6.13	3.68	1.23	*[m/s²]*
q^*	1.32	1.00	1.00	1.00	
$d^*_{e\,max}$	0.61	0.434	0.26	0.087	*[cm]*
d_{max}	0.981	**0.523**	**0.314**	**0.105**	*[cm]*
$\boldsymbol{d_u}$			**0.68**		*[cm]*

Figure 6 Left: Seismic demand spectra for Zone 3 vs capacity diagram in AD format. Right: target displacements and actual available displacements of the structure for the different zones

In figure 6, on the left, the procedure is graphically summarized for the system loaded with the modal pattern (mode 1), while in the tables at the right, the results obtained for the four seismic design zones are reported in terms of the elastic spectral acceleration, the factor q^*, the maximum inelastic displacement d^*_{max} of the equivalent system, and the maximum displacement d_u of the façade. It can be noticed that the modal load pattern (mode 1), represents the most dangerous situation, and therefore attention will be focused on this specific case, for which the assessment procedure indicates that the structure is verified for the design spectra of the zones 3 and 4. Whether $T^* \geq T_C$ or $T^* \leq T_C$, in the AD plane the inelastic demand in terms of acceleration and displacement corresponds to the intersection point of the capacity diagram with the demand spectrum corresponding to the ductility demand μ (Performance Point). Eventually, the displacement demand for the original structure is $d_{max} = \Gamma\, d^*_{max}$ and can be compared with the available ductility provided by the pushover analysis (fig. 5): $d_u = 0.818$ *cm*, for mode 1, and $d_u = 0.68$ *cm*, for mode 0.

4. FINAL REMARKS

Finally, results in terms of the two damage indices: $\Delta T\%$ (+/− the standard deviation) and the maximum mean displacement of the façade are shown in figure 7 left. In particular, for the NLD analyses, in order to perform the comparison with the pushover, a characteristic measure of the lateral acceleration was chosen for each zone, represented by the elastic spectral acceleration.

First of all, it should be remarked that there is a good agreement between the two methodologies about the limit resistance of the façade, which is identified in zone 2 by the NSP, whereas the NLD indicates that most of the zone 2 accelerograms induce the collapse. Nevertheless there are some relevant differences in the curves obtained by the two methodologies. The pushover analysis, by nature, is not much reliable for appraising the structural behaviour in the high acceleration range, where a steep damage increase occurs even for very small acceleration steps. Indeed, when

neglecting the resource given by hysteretic dissipation, the consequence is an overestimate of the induced damage. ND results, instead, are characterized by a quasi–linear trend. Indeed, for strong ground motions (Zone 2), it seems that NSP is more conservative, and provides damage indices much higher than the ND ones. Also the damage patterns obtained are more severe than the ND ones (fig. 5). On the other hand, for a low–medium seismic demand, a moderate underestimate occurs. Eventually, remembering that the sense of the NSP approach is that of providing a tool for a simplified safety assessment it can be concluded that such an objective is to some extent fulfilled. After all, the identification of a danger threshold is attained, and the corresponding displacements are in a fair good agreement with the ND simulations.

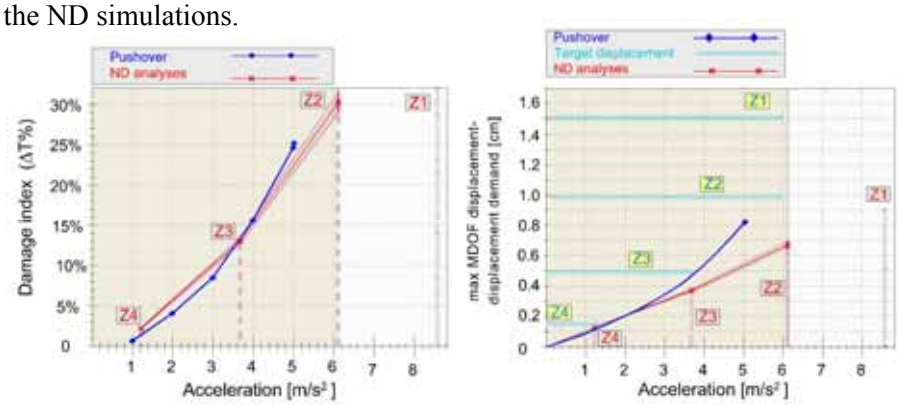

Mode 1			
Zone 1	*Zone 2*	*Zone 3*	*Zone 4*
Target Displacement (Γd^*_{max})			
1.83 cm	1.17 cm	0.56 cm	0.19 cm
Max Displacement NLD analyses			
-	0,6672	0,3716	0,1279
2.06	1.472	1.00	1.00
1.080	0.771	0.463	0.154
1.834	1.167	**0.558**	**0.186**
		0.818	

Figure 7 Comparison between Pushover and full ND analyses in terms of the global damage index *ΔT%* and the mean maximum displacement.

Granted that linear analysis methods are not advisable at all, since they are definitely too restrictive, the conclusion that can be drawn is that, if the aim is to perform a detailed safety assessment of a building, especially a monumental one, it is highly advisable to turn to NLD methods, since it is important to identify precisely the risk level: an unwarranted overestimate can lead to excessive strengthening provisions. The NSP is surely not able to provide a detailed picture of the damage extent and the nature of the collapse, and this is another reason for which in these cases it should only be used to trace a first general picture. If a large scale vulnerability assessment is to be made, NSP is definitely a good tool, since it is simple but hits the target. Nevertheless the results presented indicate the possibility

REFERENCES

[1] S. Casolo, Rigid element model for non-linear analysis of masonry façades subjected to out-of-plane loading. *Communication in Numerical Methods in Engineering*. 15(7), 457-468, 1999.
[2] S. Casolo, Modelling the out-of-plane seismic behaviour of masonry walls by rigid elements. *Earthquake Engineering and Structural Dynamics*, 29, 1797–1813, 2000.
[3] A. Corsanego, Seismic Vulnerability Evaluations for Risk Assessment in Europe. *Proc. of the 4th International Conference on Seismic Zonation*, Stanford, 1991.
[4] A. K. Chopra, R. K. Goel, Capacity–Demand–Diagram Methods Based on Inelastic Design Spectra. *Earthquake Spectra*, 15 (4), 637–656, 1999.
[5] F. Doglioni, A. Moretti, V. Petrini (eds.), *Le Chiese e il Terremoto*. Lint Press: Trieste 1994.
[6] P. Fajfar, A Nonlinear Analysis Method for Performance Based Seismic Design. *Earthquake Spectra*, 16 (3), 573–592, 2000.
[7] A. Giuffrè, A mechanical model for statics and dynamics of historical masonry buildings. In *Protection of the architectural heritage against earthquakes*, Petrini V, Save M (eds). CISM Courses and Lectures no.359. Springer-Verlag: Wien 1996.
[8] V. Petrini, Overview Report on Vulnerability Assessment. *Proc. 5th Int. Conf. on Seismic Zonation*, Nice, 1995.
[9] F. Sabetta, A. Pugliese, Estimation of Response Spectra and Simulation of Nonstationary Earthquake Ground Motion. *Bull. Seism. Soc. Am.*, 36 (2), 337–352, 1996.
[10] *Eurocode 8: Design of structures for earthquake resistance- Part 1: General rules, seismic actions and rules for buildings*.